HHS Public Access

Author manuscript

Biomaterials. Author manuscript; available in PMC 2017 January 01.

Published in final edited form as:

Biomaterials. 2016 January ; 77: 130–138. doi:10.1016/j.biomaterials.2015.10.074.

Selective binding of C-6 OH sulfated hyaluronic acid to the angiogenic isoform of $VEGF_{165}$

Dong-Kwon Lim[#a,d], **Ryan G. Wylie**[#b,d], **Robert Langer**[c], and **Daniel S. Kohane**[d,*]

[a] KU-KIST Graduate School of Converging Science and Technology, Korea University, 145 Anam-ro, Seongbuk gu, Seoul, South Korea

[b] Department of Chemistry and Chemical Biology, McMaster University, 1280 Main St. W., Hamilton, Ontario, L8S 4M1, Canada

[c] David H. Koch Institutes for Integrative Cancer Research, Massachusetts Institute of Technology, 77 Massachusetts Avenue, Cambridge, Massachusetts 02139, United States

[d] Laboratory for Biomaterials and Drug Delivery, Department of Anesthesiology, Division of Critical Care Medicine, Boston Children's Hospital, Harvard Medical School, 300 Longwood Avenue, Boston, Massachusetts 02115, United States

[#] These authors contributed equally to this work.

Abstract

Vascular endothelial growth factor 165 ($VEGF_{165}$) is an important extracellular protein involved in pathological angiogenesis in diseases such as cancer, wet age-related macular degeneration (wet-AMD) and retinitis pigmentosa. $VEGF_{165}$ exists in two different isoforms: the angiogenic $VEGF_{165a}$, and the anti-angiogenic $VEGF_{165b}$. In some angiogenic diseases the proportion of $VEGF_{165b}$ may be equal to or higher than that of $VEGF_{165a}$. Therefore, developing therapeutics that inhibit $VEGF_{165a}$ and not $VEGF_{165b}$ may result in a greater anti-angiogenic activity and therapeutic benefit. To this end, we report the selective binding properties of sulfated hyaluronic acid (s-HA). Selective biopolymers offer several advantages over antibodies or aptamers including cost effective and simple synthesis, and the ability to make nanoparticles or hydrogels for drug delivery applications or $VEGF_{165a}$ sequestration. Limiting sulfation to the C-6 hydroxyl (C-6 OH) in the *N*-acetyl-glucosamine repeat unit of hyaluronic acid (HA) resulted in a polymer with strong affinity for $VEGF_{165a}$ but not $VEGF_{165b}$. Increased sulfation beyond the C-6 OH (i.e. greater than 1 sulfate group per HA repeat unit) resulted in s-HA polymers that bound both $VEGF_{165a}$ and $VEGF_{165b}$. The C-6 OH sulfated HA (Mw 150 kDa) showed strong binding properties to $VEGF_{165a}$ with a fast association rate constant (K_a; 2.8×10^6 $M^{-1}s^{-1}$), slow dissociation rate constant (K_d; 2.8×10^{-3} s^{-1}) and strong equilibrium binding constant (K_D; ~ 1.0 nM)), which is comparable to the non-selective $VEGF_{165}$ binding properties of the commercialized therapeutic

[*]to whom correspondence should be addressed: Daniel S. Kohane M.D., Ph.D., Professor of Anaesthesia, Harvard Medical School - Boston Children's Hospital, 300 Longwood Ave. Enders 361, Boston, MA 02115, Tel: 617-919-2364, Fax: 617-730-0436, daniel.kohane@childrens.harvard.edu.

anti-VEGF antibody (Avastin®). The C-6 OH sulfated HA also inhibited human umbilical vein endothelial cell (HUVEC) survival and proliferation and human dermal microvascular endothelial cell (HMVEC) tube formation. These results demonstrate that the semi-synthetic natural polymer, C-6 OH sulfated HA, may be a promising biomaterial for the treatment of angiogenesis-related disease.

Keywords

Vascular endothelial growth factor 165; $VEGF_{165a}$; $VEGF_{165b}$; angiogenesis; sulfated sodium hyaluronate; selective binding property

1. Introduction

The ability to control the balance of angiogenic and anti-angiogenic proteins is critical for the treatment of various diseases involving pathologic angiogenesis such as solid tumor based cancers, wet age-related macular degeneration (wet-AMD) and retinitis pigmentosa, [1-4] where vascular endothelial growth factor 165 ($VEGF_{165}$) is a major angiogenic factor that enhances blood vessel formation. Therefore, $VEGF_{165}$ inhibitors have been and are currently being developed as therapeutics.[5-7]

There are two natural isoforms of $VEGF_{165}$, the angiogenic isoform $VEGF_{165a}$ and the anti-angiogenic isoform $VEGF_{165b}$.[8] Both isoforms bind VEGF receptor 2 (VEGFR2) with similar affinity but $VEGF_{165b}$ does not bind neuropilin 1 or activate downstream angiogenic signaling pathways.[8-10] Ideally, therapeutics for cancer and retinal diseases would only inhibit $VEGF_{165a}$ since $VEGF_{165b}$ has been identified as anti-angiogenic and cytoprotective. [11] The selective inhibition of $VEGF_{165a}$ could enhance treatment of angiogenic diseases where $VEGF_{165b}$ is a significant proportion of the total $VEGF_{165}$ present. It has been reported that the level of $VEGF_{165b}$ is similar to that of $VEGF_{165a}$ in diabetic retinopathy[12] and colorectal cancer.[13] In addition to its anti-antiogenic role, $VEGF_{165b}$ has been demonstrated to be a cytoprotective factor, e.g. for retinal pigmented epithelial (RPE) cells, which may be important in ocular diseases such as AMD.[11]

$VEGF_{165a}$ and $VEGF_{165b}$ both contain the same receptor-binding domain (RBD) but different heparin-binding domain (HBD) structures, which are responsible for the binding of sulfated polymers.[1] Therefore, selective $VEGF_{165a}$ binding molecules must target the HBD and not the RBD. The amino acid sequence of $VEGF_{165b}$'s HBD only differs from that of $VEGF_{165a}$ by 6 amino acids at the C-terminus, which are highlighted in red in **Fig. 1A**. This difference results in the loss of one positively charged arginine residue and a disulfide bridge in $VEGF_{165b}$.[14] The loss of the disulfide bridge results in a significant change in the three-dimensional structure of $VEGF_{165b}$'s HBD.[15] As a result, natural polysaccharides that bind the HBD such as heparan sulfate (HS) have different binding properties for $VEGF_{165a}$ and $VEGF_{165b}$.[9, 16, 17] Taking advantage of the structural differences between the HBDs, a therapeutic aptamer, pegaptanib, has been previously developed that only binds $VEGF_{165a}$.[18]

We hypothesized that selective binding to the HBD of $VEGF_{165a}$ could also be achieved by controlling the negative charge density (in this case, by sulfation) of hyaluronic acid (HA). The use of bioactive, semi-synthetic polymers prepared from HA could be a fruitful approach to controlling pathological angiogenesis because they are inexpensive, well tolerated, and stable in biological systems. Several papers have reported that sulfated HA is a potent inhibitor for tumor necrosis factor and other target proteins [16, 19-23], but sulfated HA that selectively binds $VEGF_{165a}$ over $VEGF_{165b}$ has not yet been demonstrated. HA was selected because of its biocompatibility, the structural similarities with heparin, and the chemical ability to sulfate the four hydroxy groups in each repeat unit of HA. Thus sulfated HA (s-HA) could have different degrees of sulfation (denoted s-HA-1[least sulfated], 2, 3, and 4 [most sulfated]), prepared by controlling the molar equivalents of the sulfation reagent (**Fig. 1B**). Beyond sulfation, we also investigated the effects of s-HA molecular weight (17 kDa, 150 kDa, 1,000 kDa) and different sulfate counterions (sodium, pyridine and tetrabutylammonium) on $VEGF_{165a}$ and $VEGF_{165b}$ binding (**Fig. S1**). Representative sulfated or non-sulfated naturally occurring polysaccharides were also investigated to compare their binding properties with s-HA (**Fig. S2 for structures**). Surface plasmon resonance (SPR) was used to study the binding between s-HAs and both isoforms of $VEGF_{165}$. Cell-based assays were used to evaluate the biological activity of s-HA.

2. Materials and Methods

2.1 Materials

Sodium hyaluronate (17 kDa (1.69×10^4 Da), 150 kDa (1.5×10^5 Da), 1,000 kDa (1.01×10^6 Da)) was purchased from Lifecore (Minnesota, USA). Dextran, dextran sulfate sodium salt (MW 2.0×10^5 Da , 4.0×10^5 Da), chondroitin sulfate sodium salt from bovine trachea, heparan sodium salt from bovine kidney (according to the supplier with a sulfur content of 5-7%) and monoclonal $VEGF_{165}$ antibodies (Cat. No. V4758) were purchased from Sigma-Aldrich (St. Louis, USA). Recombinant human $VEGF_{165a}$ (293-VE/CF) and $VEGF_{165b}$ (3045-VE/CF) were obtained from R&D Systems (Minneapolis, USA). The sensor chip (CM5, BR100012), amine coupling kit (BR-1000-50), running buffer (HBS-EP: 0.01 M Hepes pH 7.4, 0.15 M NaCl, 3.0 mM EDTA, 0.005% tween 20; BR100188), 10 mM glycine-HCl buffer pH 3 (BR-1003-57) and 10 mM sodium acetate buffer pH 5 (BR-1003-51) were all purchased from GE Healthcare Bio-science AB (Uppsala, Sweden). Tetrabutylammonium (TBA) hydroxide, DOWEX 50WX8-400 ion-exchange resin, sulfur trioxide pyridine complex (SO_3-pyridine, 98%), hydrazine, hydrazine sulfate, *N*-(3-Dimethylaminopropyl)-*N*′-ethylcarbodiimide hydrochloride (EDC), N-hydroxysuccinimide (NHS), dimethylformamide (DMF) and deuterated water (D_2O) were purchased from Sigma-Aldrich (St. Louis, USA). Human umbilical vein endothelial cells (HUVECs), human microvascular endothelial cells (HMVECs) purchased from Lonza (NJ, USA) and ATCC (VA, USA), respectively. Endothelial cell basal media (EBM-2 CC-3156) and endothelial cell growth media BulletKit (EGM-2 CC-3162) were purchased from Lonza (NJ, USA). CellTiter 96® AQ_{ueous} Non-Radioactive Cell Proliferation Assay (MTS assay) was purchased from Promega (WI, USA). Avastin® was purchased from Genentech/Roche (CA, USA). Getrex™ LDEV free, Calcein AM and Click-iT® EdU microplate assay were

purchased from Life Technologies (CA, USA). All images were acquired using an Olympus FSX inverted fluorescent microscope.

2.2 Methods

2.2.1 Preparation of TBA salt of HA—The preparation of tertbutylammonium hyaluronate HA (TBA-HA) of varying molecular weights (17 kDa, 150 kDa, and 1,000 kDa) was performed with the following procedure. A sodium hyaluronate solution (i.e., 150 kDa, 500 mg in 100 mL distilled water) was mixed with DOWEX 50WX8-400 ion-exchange resin (5.0 g, cation in the resin was exchanged with TBA) and stirred for 3 h. The mixture was filtered to remove the resin and freeze-dried to yield an off-white solid (TBA-HA), then analyzed with ^{1}H-NMR (**Fig. S3A**)

2.2.2 Preparation of sodium salt of sulfated HA (s-HA)—The preparation of sodium salt HA (s-HA) of varying molecular weights (17 kDa, 150 kDa, and 1,000 kDa) was performed with the following procedure. TBA-HA (off-white powder, 50 mg) was dissolved in 10 mL of N,N-dimethylformamide (DMF) and reacted with varying amounts of the sulfur trioxide pyridine complex (0.0076 g, 0.15 g, 0.38 g, and 0.61 g, respectively) dissolved in 2.0 mL of DMF to produce s-HA with 4 different sulfation degrees, hereafter referred to as s-HA-1 (least sulfated), s-HA-2, s-HA-3 and s-HA-4 (most sulfated). The reaction was conducted for 1.0 h maintaining the temperature between 0 and 5 °C while under nitrogen. The reaction was quenched by adding 10 mL of water, and the pH of the solution was adjusted to 8.5 - 9.0 with a 1.0 M NaOH solution producing the sodium salt of sulfated HA. The samples were then dialyzed against distilled water for 3 days. Finally, the samples were lyophilized to yield off-white solids (obtained: s-HA-1 (36 mg), s-HA-2 (42.8 mg), s-HA-3 (47.8 mg), s-HA-4 (51.5 mg). The products were characterized by ^{1}H, ^{13}C-NMR and zeta potential analysis (**Figs. 1A & S3B**).

2.2.3 Preparation of pyridine and TBA salt of sulfated HA (Pyr/TBA-s-HA)—The pyridine and TBA salt of sulfated HA with varying molecular weights (17 kDa, 150 kDa, and 1,000 kDa) was prepared by performing the following procedure. TBA-HA (off-white powder, 50 mg) was dissolved in 10 mL of N,N-dimethylformamide (DMF) and reacted with varying amounts sulfur trioxide pyridine complex (SO_3-pyridine) in 2.0 mL of DMF (0.0076 g, 0.15 g, 0.38 g, and 0.61 g, respectively) while maintaining temperature between 0 and 5 °C while under nitrogen for 1.0 h. The reaction progress was quenched by adding 10 mL of water without additional pH adjustment step. The solution was dialyzed against distilled water for 3 days. The samples were lyophilized to yield off-white solids (Pyr/TBA-s-HA).

2.2.4 Preparation of fully sulfated chondroitin (CS-2)—Sodium salt chondroitin sulfate A (500 mg, CS-1) from bovine trachea was first converted into TBA salt of chondroitin (TBA-CS-1) by following the same method for TBAHA preparation. The lyophilized TBA-CS-1 (100 mg) was suspended in DMF (20 mL) under nitrogen at room temperature and cooled to 0 - 5 °C. Sulfur-trioxide pyridine complex solution (1.2 g/20 mL) in DMF was added into the TBA-CS-1 solution, then stirred for 1.0 h at 0 ~ 4 °C. After quenching the reactions with water (10 mL), the pH of the solution was adjusted to be

between 9 and 10 using a 1.0 M NaOH solution. The solution was then purified by dialysis against distilled water, followed by lyophilization (See **Fig. S2** for structures).

2.2.5 Preparation of sodium salt of N-deacetylated s-HA-2 (deacetyl-s-HA)— Pyr/TBA salt of s-HA-2 (1,000 kDa, 200 mg) was suspended in DMF (20 mL) under nitrogen at room temperature. Hydrazine (20 mL) and hydrazine sulfate (200 mg) were added, and the reaction mixture was stirred for 4.0 h at ~100 °C, cooled to room temperature and the pH adjusted at 9 - 10 with 2.0 M NaOH solution. The mixtures were concentrated to dryness and then dissolved in water (50 mL) and acetone (50 mL), followed by dialysis against water and lyophilization. The product was characterized by ^{1}H-NMR (D_2O) analysis (**Figs. S1 & S3C**).

2.2.6 Surface plasmon resonance-based binding studies of polymer and $VEGF_{165}$—We used surface plasmon resonance (SPR) based method to investigate the binding affinity of all polymers and antibodies for $VEGF_{165a}$ and/or $VEGF_{165b}$. SPR-based detection allows for label free solution state monitoring of binding interactions between proteins and biomolecules, which can provide quantitative measurements of binding and dissociation kinetics.[22] In this case, the protein ($VEGF_{165a}$ or $VEGF_{165b}$) is immobilized onto a thin gold membrane surface through well-established chemistry, and then a solution containing polymers (i.e. s-HA) or antibodies (i.e. anti-VEGF) is flowed over the protein modified surface to obtain sensorgram.

2.2.7. Immobilization of $VEGF_{165a}$ or $VEGF_{165b}$ on CM5 biosensor chip surfaces—A BIAcore 3000 instrument with BIAcore Control and BIAevaluation software 4.1 from GE Healthcare (Uppsala, Sweden) was used.[23, 24] $VEGF_{165a}$ or $VEGF_{165b}$ was immobilized onto the carboxymethylated dextran coated gold membrane surface on the CM5 biosensor chip. In brief, the carboxymethylated dextran coated surface was activated with EDC/NHS. Protein immobilization was accomplished by injecting 700 μL of 10 μg/mL $VEGF_{165a}$ or $VEGF_{165b}$ in 10 mM sodium acetate buffer at pH 5.5. The unreacted activated carboxylic acids on the chip surface were blocked with a 35 μL injection of 1.0 M ethanolamine-HCl (pH 8.5). The chip was then washed with a continuous flow of the HBS-EP running buffer (0.01 M HEPES pH 7.4, 0.15 M NaCl, 3.0 mM EDTA, 0.005% tween 20).

2.2.8 SPR measurements for sulfated polysaccharide interactions with $VEGF_{165a}$ or $VEGF_{165b}$—Each s-HA powder was dissolved in HBS-EP running buffer. The solutions were flowed over the surface of the VEGF modified chip using the auto-injector according to the following procedure: 1) Running buffer was flowed for 1 minute; 2) Sample solutions were injected for 3.0 min at 30 μL/min (association phase); 3) Running buffer was flowed for 2.0 min (dissociation phase); 4) 30 μL of 3.0 M NaCl was injected to remove bound polymers from the chip surface (regeneration phase); 5) The system was re-equilibrated by flowing HBS-EP running buffer for 2.0 minutes before repeating the procedure for the next sample. The SPR response was monitored as a function of time at 25 °C and subtracted from the response of a reference control chip that did not contain VEGF. Kinetic parameters were evaluated using the BIA evaluation software 4.1.

2.2.9 SPR measurements for anti-VEGF antibody interactions with $VEGF_{165a}$ or $VEGF_{165b}$—The same procedure was used as in 2.2.8 except that the regeneration phase consisted of a 30 μL injection of a 10 mM glycine-HCl buffer a pH 3 instead of a 3.0 M NaCl solution.

2.2.10 HUVEC viability assay—Human umbilical vein endothelial cells (HUVEC) (ATCC, USA) were used from passages 3 to 5. To assess HUVEC viability in full growth medium, HUVECs in EGM-2 were seeded into 96-well plates (10 k cells/well) and incubated at 37 °C – 5% CO_2. After one day, the media was changed to EGM-2 that contained the prepared sulfated HA or Avastin® solutions. After 1 day, HUVEC viability was assessed by use of the MTS assay (Promega, USA). All samples were normalized to controls that did not contain any polymers or Avastin®.

2.2.12 HMVEC tube-formation assay (2D)—Cold Geltrex™ (Invitrogen, USA) solution at 4 °C was pipetted into 96-well plates (80 μL/well). Geltrex™ solutions were gelled by incubating the plates at 37 °C for 1.0 h. HUVECs in EBM-2 medium with 0.5% FBS, and 100 ng/mL of $VEGF_{165a}$ were seeded into the Geltrex™ -coated 96-well plate (15 k cells/well). Different samples to be tested were then added (HA, s-HA-2, HS and Avastin®). The cells were incubated for 24 h. The cells were stained with Calcein AM (Life technologies, USA) for visualization. Images were acquired using an inverted fluorescent microscope. Branch points of HUVEC tube were manually counted based on the images.

3. Results and Discussions

3.1 Synthesis and Characterization of Sulfated Hyaluronic Acid (s-HA)

s-HAs were synthesized by reacting HA with sulfur trioxide pyridine complex using previously reported methods.[19, 22] We synthesized a variety of s-HAs with different molecular weights (MW; 17, 150 and 1,000 kDa) and degrees of sulfation. The degree of sulfation was controlled by the addition of different molar ratios of sulfur trioxide pyridine complex per repeat unit of HA. The ratios of moles of sulfur trioxide pyridine complex to moles of HA repeat units were 1:1, 2:1, 5:1 or 8:1 which we termed s-HA-1 (least sulfated), s-HA-2, s-HA-3 or s-HA-4 (most sulfated) respectively. Sulfation of HA occurs at hydroxyl groups, i.e. at C-2', C-3', C-4, or C-6 OH in **Fig. 1B**, where R can represent either H or SO_3^- depending on the degree of sulfation. Sulfation would occur first at the C-6 position since it is the only primary and most reactive hydroxyl in HA.

^{1}H-NMR and ^{13}C-NMR analysis were performed to determine the degree of sulfation of each s-HA. Representative data for s-HAs prepared from 150 kDa HA are shown in **Fig. 1C-D**. Sulfation of C-6 OH, the most reactive hydroxyl, could be followed by ^{1}H-NMR since it resulted in the downfield shift of the C-6 CH_2 protons from 3.45 ppm to 3.55 ppm due to higher electron withdrawing properties of sulfate groups (**Fig. 1C**).[22, 25] ^{1}H-NMR showed that s-HA-1 was only partially sulfated at the C-6 position since peaks were observed at both 3.45 and 3.55 ppm (red arrow). Complete sulfation at C-6 was achieved for s-HA-2, s-HA-3 and s-HA-4 since no peak was observed at 3.45 ppm and a new peak was detected at 3.55 ppm (blue arrow). s-HA-3 and s-HA-4 showed new peaks in the range of 3.9 ~ 4.4 ppm (green arrows) indicating additional hydroxyl sulfation at positions C-2', C-3'

and C-4. Since these positions are all secondary hydroxyls and thus have similar reactivity, s-HA-3 and s-HA-4 both contained a mixture of degrees of sulfation at those positions. The increased relative peak heights between 3.9 ~ 4.4 ppm for s-HA-4 compared to s-HA-3 indicated a higher degree of sulfation.

In **Fig. 1D**, the ^{13}C peak at 61.1 ppm represents the C-6 carbon in unmodified HA. Sulfation of the OH at C-6 resulted in a peak shift from 61.1 to 67.7 ppm (blue arrow).[25] Since peaks were observed at both 61.1 and 67.7 ppm in s-HA-1, we can conclude that the C-6 position was partially sulfated. HAs with increased sulfation (s-HA-2, s-HA-3 and s-HA-4) were completely sulfated at the C-6 position, as seen by the complete disappearance of the peak at 61.1 ppm.

Sulfation of HA resulted in an increase in negative charge density, as reflected in the decreasing zeta potential with increasing sulfation (**Fig. 1E**), from −21 ± 5 mV for HA to −45 ± 3 mV for s-HA-4. Increased sulfation of HA also decreased the pH of aqueous s-HA solutions (1.0 mg/mL). The pH of HA, s-HA-1, s-HA-2, s-HA-3, and s-HA-4 solutions were 6.05, 5.55, 4.33, 4.25, and 4.15 respectively.

3.2 Selective Binding Properties and Structure Relationship

To study the binding properties of s-HA to $VEGF_{165a}$ and $VEGF_{165b}$ we performed surface plasmon resonance (SPR)-based binding studies. A chip with a thin gold film coated with carboxymethylated dextran was covalently modified with either $VEGF_{165a}$ or $VEGF_{165b}$ using EDC/NHS chemistry (**Fig. 2A**). [23, 24] Each s-HA solution was injected and flowed over the surface of the chip modified with $VEGF_{165a}$ or $VEGF_{165b}$. A change in SPR signal was observed if the polymers bound to the immobilized protein, from which binding kinetics were calculated. All experiments were performed using the same concentrations of polymer (50 μg/mL) and the change of SPR signal was recorded as a relative intensity of binding response (SPR signal in arbitrary units, a. u.) over time for each sample (**Fig. 2A**). We investigated the binding response of HA and s-HAs to $VEGF_{165a}$ (black bar) and $VEGF_{165b}$ (empty bar) at 200 msec after injection with respect to sulfation degree (s-HA-1, s-HA-2, s-HA-3, and s-HA-4), molecular weight (17 kDa, 150 kDa, 1,000 kDa), and counter cations (sodium in **Fig. 2B-D**, Pyr/TBA salt in **Fig. 2E-G**; sensorgrams for those data are in **Figs. S4-S6**). All samples were compared to HA of the same molecular weight to determine if statistically significant binding occurred. As shown in **Fig. 2B-G**, relatively weak SPR responses (i.e. no binding to VEGF) were observed for unmodified HA or s-HA-1 regardless of molecular weight and types of counter cation for binding to either $VEGF_{165a}$ (black bar) or $VEGF_{165b}$ (empty bar). Importantly, all molecular weights of the sodium salt (X=Na) of s-HA-2 studied showed strong binding responses for $VEGF_{165a}$ but not $VEGF_{165b}$, indicating selective binding (**Fig. 2B-D**; unpaired t tests $p < 0.05$). The binding response of 17 kDa and 150 kDa s-HA-2 for $VEGF_{165b}$ was not significantly different from those of 17 kDa and 150 kDa HA (unpaired t test, $p > 0.05$), indicating the sulfate groups in s-HA-2 did not increase its affinity for $VEGF_{165b}$. The binding response of 1000 kDa s-HA-2 for $VEGF_{165b}$ was significantly stronger than that of 1000 kDa HA for $VEGF_{165b}$ (unpaired t test, $p < 0.05$), indicating that sulfation of 1000 kDa HA did result in a small increase in affinity for $VEGF_{165b}$. s-HAs with higher degrees of sulfation (s-HA-3 and s-HA-4) showed

even stronger binding responses for $VEGF_{165a}$ but also bound $VEGF_{165b}$ when compared to HA (unpaired t tests, $p < 0.05$). Therefore, only s-HA-2 had the appropriate sulfation degree for selective binding of $VEGF_{165a}$ (**Fig. 2B-D)**. The binding response of s-HAs to VEGF increased as a function of s-HA MW, this may be attributable to the fact that SPR binding responses are proportional to the mass of the bound molecule (**Fig. 2B-D**).[26] The tetrabutylammonium (TBA) and pyridine salts of s-HA (17, 150, 1000 kDa) showed a lower binding response for $VEGF_{165a}$ than did the sodium salt of s-HA (X=Na) as shown in **Fig. 2B-C, E-F** (unpaired t tests, $p < 0.05$). A decrease in binding was also observed for TBA and pyridine salts of s-HA for $VEGF_{165b}$ as compared to the sodium salt of s-HA for 17 and 150 kDa s-HA-3 and s-HA-4, and 1000 kDa s-HA-2, s-HA-3 and s-HA-4 (unpaired t tests, $p < 0.05$). 17 and 150 kDa s-HA-1 and s-HA-2 and 1000 kDa s-HA-1 did not show any significant binding to $VEGF_{165b}$ when compared to HA (unpaired t tests, $p > 0.05$), and therefore did not show a difference in binding when comparing s-HA with different counter ions. The lower binding responses with the TBA and pyridine salts of s-HA may be attributable to increased steric hindrance from the larger counter cations during polymer-protein complex formation. We also investigated if other common polysaccharides with various degrees of sulfation have selective binding properties for $VEGF_{165a}$ (**Fig. S2** for structures). None of the investigated sulfated polymers except s-HA-2 showed selective binding to $VEGF_{165a}$. Dextran (non-sulfated; Dex) showed no detectable response to either isoform of $VEGF_{165}$, whereas sulfated dextran (s-Dex; 200 kDa and 400 kDa; 2.3 sulfate groups per glucosyl residue) showed strong binding responses to both $VEGF_{165a}$ and $VEGF_{165b}$ (**Fig. 3A, S7**). The binding response of s-Dex for $VEGF_{165a}$ was only 1.1 times stronger than that for $VEGF_{165b}$ (**Fig. 3A**). Heparan sulfate (HS), which has variable sulfations at C-2', C-3', and C-6 OH, bound both $VEGF_{165a}$ and $VEGF_{165b}$ (**Figs. 3A, S7**). [20] Heparan sulfate's binding response for $VEGF_{165b}$ was approximately half that for $VEGF_{165a}$, which is consistent with a previous report.[20] Chondroitin sulfate (CS-1), C-4 OH sulfated (**Fig. S2**), showed very weak SPR responses to both isoforms of $VEGF_{165}$, while completely sulfated chondroitin (CS-2; **Fig. S2**), where all hydroxyls are sulfated, showed strong binding responses to both isoform of $VEGF_{165}$ (**Figs. 3B, S8**). CS-2 bound $VEGF_{165a}$ with twice the intensity as $VEGF_{165b}$ (**Fig. 3B**). The binding behaviors of HS and CS-2 for both isoforms of $VEGF_{165}$ were similar to those of the highly sulfated HAs, s-HA-3 and s-HA-4. s-HA-2 was the only polymer studied here that was found to have selective binding to $VEGF_{165a}$. One possible implication is that a specific degree of sulfation is critical for selective binding.

To further demonstrate that the total charge density is important for the selective binding properties of s-HA-2, a new positive charge was introduced by removing the acetyl group in the N-glucosamine unit of HA and the effect on binding behaviors was studied. N-deacetylated s-HA-2 (deacetyl s-HA) was synthesized by reducing the acetyl group to an amine (positive charge) with hydrazine. Deacetylated s-HA-2 showed a 4 fold decrease in binding response for $VEGF_{165a}$ compared to s-HA-2 (**Figs. 2C, 3B, S8**). The decreased binding response of deacetyl s-HA was most likely due to the introduction of a positively charged amine group at C-2 (**Fig. 1B**), which supports the importance of charge density for selective binding.

Since Avastin®, an anti-VEGF antibody, is the current clinical standard for VEGF binding and inhibition, we studied its binding profile to $VEGF_{165a}$ and $VEGF_{165b}$. Avastin® is known to bind the receptor binding domain that is present in both $VEGF_{165a}$ and $VEGF_{165b}$. The SPR study used to evaluate s-HA-2 binding showed a strong binding response of Avastin® for both isoforms of $VEGF_{165}$ (**Fig. 3B)**, which is consistent with a prior report. [13]

To compare the affinities of the various agents, their binding kinetics and rate constants for $VEGF_{165a}$ and $VEGF_{165b}$ were calculated (Table 1) from SPR binding experiments at multiple concentrations for each agent (**Figs. 3C-D, S9, S10**). The binding constants were calculated using the Langmuir binding model.[27] Avastin® and the sulfated polymers other than s-HA-2 showed similar association and dissociation rate constants (k_a and k_d respectively) for both isoforms of VEGF. The slightly higher $VEGF_{165a}$ association rate constants for sulfated polysaccharides compared to Avastin® may be attributable to the presence of multiple binding sites in polymers.[28] The binding rate constants of s-HA-2 for $VEGF_{165a}$ were similar to those of the other molecules, but it did not bind $VEGF_{165b}$ and therefore did not have binding rate constants for that molecule (**Fig. 3C, Table 1**). The data demonstrated that s-HA-2 was able to bind $VEGF_{165a}$ with affinity similar to that of Avastin® and other sulfated polymers, but was unique for its selective binding properties.

3.3 *In vitro* bioactivity of s-HA-2

The anti-angiogenic activity of s-HA-2 prepared from HA (MW 150 kDa) was studied because of its selective and strong binding affinity for $VEGF_{165a}$. The inhibition of $VEGF_{165a}$ by s-HA-2 was evaluated by examining the effects of s-HA-2 on the viability of human umbilical vein endothelial cells (HUVECs) in endothelial growth media (EGM-2) which contains endothelial basal media (EBM-2), $VEGF_{165a}$, 2% FBS, FGF-2, and EGF (**Fig. 4A**). Cell viability (using the CellTiter 96® Aqueous Solution Cell Proliferation Assay [MTS]) was measured in the presence of HA, s-HA-2, and Avastin® at the concentrations 0, 1.0, 10, 100, and 1,000 μg/mL since HS, a similar polymer to s-HA-2, was previously shown to inhibit $VEGF_{165a}$ in this concentration range.[29] All data were normalized to those from cells grown in EGM-2 without HA, s-HA-2 and Avastin® (dashed line at 100, **Fig 4A**). s-HA-2 showed a significant decrease in cell viability when compared to samples with HA or Avastin® at all concentrations studied (2 way ANOVA with bonferroni correction, $p < 0.05$). To further examine the inhibitory effect of s-HA-2, we performed tube formation assays with human dermal microvascular endothelial cells (HMVECs) on Geltrex™ coated surfaces in EBM-2 media with 0.5% FBS and $VEGF_{165a}$ (100 ng/mL). FGF-2 and EGF were not included to isolate the effects of s-HA-2 on $VEGF_{165a}$. Several different conditions were studied: a negative control that did not contain $VEGF_{165a}$; a positive control that contained $VEGF_{165a}$; HA (100 or 1000 μg/mL) with $VEGF_{165a}$; s-HA-2 (100 and 1000 μg/mL) with $VEGF_{165a}$; and, Avastin® (100 μg/mL) with $VEGF_{165a}$ (**Fig. 4B-C**). For quantification, the number of branch points in images acquired from 4 independent samples per condition were counted, compared with a 1-way ANOVA with Bonferroni's correction. The positive controls with $VEGF_{165a}$ contained more branch points than the negative control without $VEGF_{165a}$. Only HA at 100 μg/mL was not significantly different from the positive control, indicating that all other samples inhibited tube formation. The inhibitory effect of

HA at 1 mg/mL ($p < 0.05$) indicated that high concentrations of non-sulfated polymers may interfere with tube formation. Both s-HA-2 and Avastin® at 100 μg/mL were significantly lower than the positive control ($p < 0.05$) but not from each other ($p > 0.05$).

4. Discussion

Several cancers and common retinal diseases involve $VEGF_{165a}$-induced pathological angiogenesis. Consequently, it is important to develop anti-angiogenic therapeutics that target $VEGF_{165a}$ and not the anti-angiogenic isoform $VEGF_{165b}$ that is prevalent in some diseases. This work demonstrated that HA modified with sulfate groups at the C-6 hydroxyl group (s-HA-2) selectively bound the angiogenic isoform of VEGF, $VEGF_{165a}$. Previously, selective binding of $VEGF_{165a}$ has only been accomplished with the aptamer pegaptanib (Macugen®), which has a similar K_D for $VEGF_{165a}$ as s-HA-2 (0.2 nM for pegaptanib and 1 nM for s-HA-2).[6] The use of selective biopolymers as $VEGF_{165a}$ inhibitors has several advantages over aptamers: 1) raw materials are relatively cheap, 2) synthesis and purification are simple, and 3) nanoparticles and hydrogels can be made from those materials for long-term drug delivery applications or sequestration agents (e.g. a $VEGF_{165a}$ sponge).

It was determined that 1 sulfate group per repeat unit of HA resulted in selective binding for $VEGF_{165a}$. Since HA's repeat unit has 1 primary hydroxyl and primary hydroxyls are more reactive than secondary hydroxyls, sulfation was easily limited to the primary hydroxyl by controlling the ratio of sulfation reagent to HA (as with s-HA-2). Increasing the ratio of sulfation reagent to HA results in the complete sulfation of HA's primary hydroxyl and a mixture of sulfated secondary hydroxyls, resulting in non-selective s-HAs (e.g. s-HA-3 and s-HA-4). Other polysaccharides such as dextran and chondroitin only contain secondary hydroxyls, making it difficult to limit sulfation to 1 sulfate group per repeat unit.

s-HA-2's and the natural polymer HS both bound $VEGF_{165a}$ (K_D of 1.0 and 3.3 nM for s-HA-2 and HS, respectively; **Fig 3, Table 1**) but only HS bound $VEGF_{165b}$. This indicates that the binding strength of a sulfated polymer for $VEGF_{165a}$ does not predict its binding strength for $VEGF_{165b}$. Therefore, the difference in binding affinity of sulfated polymers for $VEGF_{165a}$ and $VEGF_{165b}$ was not only dependent on the negative charge density, but may involve other non-covalent interactions. Highly sulfated polymers such as s-HA-3, s-HA-4, s-Dex, and CS-2 were shown to strongly bind both VEGF isoforms mostly likely due to the large number of possible ionic interactions. The total binding ability of s-HA-2 can be calculated from its K_D, which will determine if s-HA-2 can be used as a sink for $VEGF_{165a}$ for various diseases. Since most retinal and cancer diseases have $VEGF_{165a}$ concentrations similar to or below the K_D of s-HA-2 for $VEGF_{165a}$ (1 nM), 50% of $VEGF_{165a}$ will be bound when the concentration of s-HA-2 is equal to s-HA-2's K_D (1 nM). 100% of $VEGF_{165a}$ will be bound when the concentration of s-HA-2 is equal to 100 times the K_D of s-HA-2 (100 nM).

Unlike Avastin®, s-HA-2 blocks $VEGF_{165a}$ activity by binding to the HBD and not the RBD.[30] Other molecules such as heparan sulfate[29] and pegaptanib[31] that bind the HBD have also been demonstrated to be $VEGF_{165a}$ inhibitors. Inhibition is believed to occur

through 2 different mechanisms: 1) steric hindrance; and, 2) prevention of $VEGF_{165a}$ binding to HS coated cell surfaces. The binding of sulfated polymers or the PEGylated aptamer, pengaptanib, to the HBD of $VEGF_{165a}$ is believed to sterically interfere with $VEGF_{165a}$ complexation with cell surface receptors.[31] HS on the surface of cells is believed to locally enhance the concentration of $VEGF_{165a}$, which in turns increases the rate of VEGF receptor activation. HBD competitors such as s-HA-2 could decrease the concentration of $VEGF_{165a}$ on the cell surface through sequestration of soluble $VEGF_{165a}$ and therefore decrease the rate of VEGF receptor activation.[31]

s-HA-2 differs from Avastin since it targets the HBD, and therefore will most likely bind all cytokines that contain a HBD, whereas Avastin binds VEGF isoforms with the VEGFR2 receptor binding domain. Therefore, s-HA-2 may prove beneficial over Avastin when the binding of other growth factors with HBDs is needed. For instance, FGF-2, which contains a HBD, has been shown to enhance proliferation of human pancreatic cancer.[32] We confirmed experimentally that s-HA-2 does indeed bind FGF-2 (**Fig. S13**). Conversely, Avastin® may be beneficial when only VEGF proteins should be targeted. The choice of therapeutic for specific diseases will depend on the therapeutic targets.

Since s-HA-2 binds $VEGF_{165a}$'s HBD, it most likely inhibits $VEGF_{165a}$ activity in a similar manner to other therapeutics that bind the HBD of $VEGF_{165a}$ such as pegaptanib. Pegaptanib prevents the binding of $VEGF_{165a}$ to NP-1 by blocking the HBD and limits neovascularization.[33] The binding of $VEGF_{165a}$'s HBD to NP-1 enhances the $VEGF_{165a}$-VEGFR2 interaction and leads to increase neovascularization. The introduction of soluble heparan sulfate at high concentrations also decreases the activity of $VEGF_{165a}$, which is also believed to be the result of decreased NP-1 activation and prevention of $VEGF_{165a}$ sequestration near the cellular surface.[34] Therefore, it is likely that s-HA-2 will limit $VEGF_{165a}$ neovascularization in a similar manner as pegaptanib and heparan sulfate. I In a manner similar to growth factors bound to the ECM [35], $VEGF_{165a}$ bound to s-HA-2 might still be degraded by plasmin into smaller VEGF isoforms that do not have a HBD, and which therefore would no longer interact with s-HA-2.

To limit potential systemic side effects, as with any therapy, s-HA-2 could be administered directly at the disease sites (e.g. injection into the eye to treat retinal degenerative diseases) or incorporated into delivery vehicles (e.g.,s-HA-2 within cancer-targeting nanoparticles). If s-HA-2 is injected systemically without a delivery vehicle, it could have adverse effects in regions that require $VEGF_{165a}$ activity. s-HA-2 may have other biological effects; for example it could activate HA signaling pathways such as CD44 receptor activation.

s-HA-2 was designed to be a heparan sulfate mimic to bind HBDs, and therefore may influence the composition of the native extracellular matrix (ECM). The introduction of s-HA-2 will effectively increase the amount heparan sulfate like polymers in the extracellular matrix (ECM). This may lead to a greater sequestration of heparin binding growth factors, which may result in a rapid release of growth factors in a short time period when the ECM is degraded. Therefore, it will be important to limit the delivery s-HA-2 to disease sites.

In growth media conditions that contain 2% FBS, EGF, FGF-2 and $VEGF_{165a}$, s-HA-2 hindered HUVEC viability to a greater extent than did HA or Avastin® at all concentrations tested (1 to 1000 μg/mL, **Fig 4A**, $p < 0.05$). HA was not expected to influence HUVEC proliferation or survival since it does not bind growth factors. Avastin® did not show a significant decrease in HUVEC viability (**Fig 4A**). Since Avastin® is specific for $VEGF_{165}$ [36], it is only capable of blocking $VEGF_{165}$ activity and not the multiple other factors present in growth media. s-HA-2 is probably able to bind and sequester growth factors with HBDs and thus interfere with several other pathways (e.g., FGF-2). To determine the effects of $VEGF_{165a}$ inhibition, a HMVEC tube formation assay was performed in media with 0.5% FBS and 100 ng/mL $VEGF_{165a}$. Both s-HA-2 and Avastin® (100 μg/mL) decreased tube formation when compared to the positive control ($p < 0.05$), but were not significantly different from each other ($p > 0.05$, **Fig 4B**). High concentration of HA (1 mg/mL also hindered the tube formation even though it does not bind growth factors. We expect s-HA-2 to show similar anti-$VEGF_{165a}$ inhibition to heparan sulfate since they both bind the same site (HBD of $VEGF_{165a}$) and have similar K_D (1.0 and 3.3 nM for s-HA-2 and heparan sulfate respectively). Heparan sulfate has been show to inhibit endothelial cell migration and tube formation as well as limit angiogenic activity in in vitro and in vivo models.[34]

5. Conclusion

We demonstrated the strong ($K_D \sim 1.0$ nM) and selective binding properties of C-6 OH sulfated sodium hyaluronate (s-HA-2) to $VEGF_{165a}$ with a label-free real-time assay (SPR). Structurally similar sulfated polysaccharides did not have $VEGF_{165a}$ selective binding properties. The degree of sulfation was critical for selective binding. Only s-HA with 1 sulfate group per repeat unit showed selective binding. Cell viability and tube formation assays in various media conditions with $VEGF_{165a}$ demonstrated that s-HA-2 does inhibit $VEGF_{165a}$ activity. This indicates the potential of s-HA-2 as a therapeutic to treat angiogenesis-related diseases.

Supplementary Material

Refer to Web version on PubMed Central for supplementary material.

Acknowledgements

This work was supported by grants from Sanofi-Aventis, NIH Grant # DE013023 (R.L.) and NIH Grant # GM073626 (D.S.K). RGW also thanks the support of the Banting Postdoctoral Fellowship from the Natural Sciences and Engineering Research Council of Canada.

References

1. Ferrara N. Vascular endothelial growth factor and age-related macular degeneration: from basic science to therapy. Nat Med. 2010; 16:1107–11. [PubMed: 20930754]
2. Witmer AN, Vrensen G, Van Noorden CJF, Schlingemann RO. Vascular endothelial growth factors and angiogenesis in eye disease. Prog Retin Eye Res. 2003; 22:1–29. [PubMed: 12597922]
3. Folkman J, Langer R, Linhardt RJ, Haudenschild C, Taylor S. Angiogenesis inhibition and tumor-regression caused by heparin or a heparin fragment in the presence of cortisone. Science. 1983; 221:719–25. [PubMed: 6192498]

4. Folkman J, Bach M, Rowe JW, Davidoff F, Lambert P, Hirsch C, et al. Tumor angiogenesis - therapeutic implications. N Engl J Med. 1971; 285:1182–6. [PubMed: 4938153]
5. Andreoli CM, Miller JW. Anti-vascular endothelial growth factor therapy for ocular neovascular disease. Current opinion in ophthalmology. 2007; 18:502–8. [PubMed: 18163003]
6. Ng EW, Shima DT, Calias P, Cunningham ET, Guyer DR, Adamis AP. Pegaptanib, a targeted anti-VEGF aptamer for ocular vascular disease. Nature reviews drug discovery. 2006; 5:123–32. [PubMed: 16518379]
7. Ferrara N. VEGF as a therapeutic target in cancer. Oncology. 2005; 69:11–6. [PubMed: 16301831]
8. Bates DO, Cui TG, Doughty JM, Winkler M, Sugiono M, Shields JD, et al. VEGF(165)b, an inhibitory splice variant of vascular endothelial growth factor, is down-regulated in renal cell carcinoma. Cancer Res. 2002; 62:4123–31. [PubMed: 12124351]
9. Nowak DG, Woolard J, Amin EM, Konopatskaya O, Saleem MA, Churchill AJ, et al. Expression of pro- and anti-angiogenic isoforms of VEGF is differentially regulated by splicing and growth factors. J Cell Sci. 2008; 121:3487–95. [PubMed: 18843117]
10. Woolard J, Wang WY, Bevan HS, Qiu Y, Morbidelli L, Pritchard-Jones RO, et al. VEGF(165)b, an inhibitory vascular endothelial growth factor splice variant: Mechanism of action, in vivo effect on angiogenesis and endogenous protein expression. Cancer Res. 2004; 64:7822–35. [PubMed: 15520188]
11. Magnussen AL, Rennel ES, Hua J, Bevan HS, Long NB, Lehrling C, et al. VEGF-A165b Is Cytoprotective and Antiangiogenic in the Retina. Investigative Ophthalmology & Visual Science. 2010; 51:4273–81. [PubMed: 20237249]
12. Willis J, Scott R, Darlow B, Campbell-Stokes PL, Taylor BJ, on behalf of the New Zealand Children's Diabetes Working Group. Prospective incidence study of diabetes mellitus in New Zealand children aged 0 to 14 years. Diabetologia. 2005; 48:643–648. [PubMed: 15759108] Diabetologia. 2005; 48:2442–3. [PubMed: 16195865]
13. Varey A, Rennel E, Qiu Y, Bevan H, Perrin R, Raffy S, et al. VEGF165b, an antiangiogenic VEGFA isoform, binds and inhibits bevacizumab treatment in experimental colorectal carcinoma: balance of pro-and antiangiogenic VEGF-A isoforms has implications for therapy. British journal of cancer. 2008; 98:1366–79. [PubMed: 18349829]
14. Robinson CJ, Mulloy B, Gallagher JT, Stringer SE. VEGF(165)-binding sites within heparan sulfate encompass two highly sulfated domains and can be liberated by K5 lyase. Journal of Biological Chemistry. 2006; 281:1731–40. [PubMed: 16258170]
15. Harper SJ, Bates DO. VEGF-A splicing: the key to anti-angiogenic therapeutics? Nature Reviews Cancer. 2008; 8:880–7. [PubMed: 18923433]
16. Grunewald FS, Prota AE, Giese A, Ballmer-Hofer K. Structure-function analysis of VEGF receptor activation and the role of coreceptors in angiogenic signaling. BBA-Proteins Proteomics. 2010; 1804:567–80. [PubMed: 19761875]
17. Dejima K, Kleinschmit A, Takemura M, Choi PY, Kinoshita-Toyoda A, Toyoda H, et al. The role of drosophila heparan sulfate 6-O-endosulfatase in sulfation compensation. Journal of Biological Chemistry. 2013; 288:6574–82. [PubMed: 23339195]
18. Magnussen AL, Rennel ES, Hua J, Bevan HS, Long NB, Lehrling C, et al. VEGF-A165b is cytoprotective and antiangiogenic in the retina. Investigative ophthalmology & visual science. 2010; 51:4273–81. [PubMed: 20237249]
19. Benitez A, Yates TJ, Lopez LE, Cerwinka WH, Bakkar A, Lokeshwar VB. Targeting hyaluronidase for cancer therapy: Antitumor activity of sulfated hyaluronic acid in prostate cancer cells. Cancer Res. 2011; 71:4085–95. [PubMed: 21555367]
20. Cole CL, Hansen SU, Barath M, Rushton G, Gardiner JM, Avizienyte E, et al. Synthetic heparan sulfate oligosaccharides inhibit endothelial cell functions essential for angiogenesis. PLoS One. 2010:5.
21. Hacker U, Nybakken K, Perrimon N. Heparan sulphate proteoglycans: The sweet side of development. Nat Rev Mol Cell Biol. 2005; 6:530–41. [PubMed: 16072037]
22. Hintze V, Moeller S, Schnabelrauch M, Bierbaum S, Viola M, Worch H, et al. Modifications of hyaluronan influence the interaction with human bone morphogenetic protein-4 (hBMP-4). Biomacromolecules. 2009; 10:3290–7. [PubMed: 19894734]

23. Chang NS, Intrieri C, Mattison J, Armand G. Synthetic polysulfated hyaluronic acid is a potent inhibitor for tumor necrosis factor production. Journal of Leukocyte Biology. 1994; 55:778–84. [PubMed: 8195703]
24. Chang N-S. Hyaluronidase induces murine L929 fibrosarcoma cells resistant to tumor necrosis factor and fas cytotoxicity in the presence of actinomycin D. Cell Biochem Biophys. 1995; 27:109–32. [PubMed: 9106395]
25. Magnani A, Lamponi S, Rappuoli R, Barbucci R. Sulphated hyaluronic acids: a chemical and biological characterisation. Polymer International. 1998; 46:225–40.
26. Schasfoort RB, Tudos AJ. Handbook of surface plasmon resonance: Royal Society of Chemistry. 2008
27. Maynard HD, Hubbell JA. Discovery of a sulfated tetrapeptide that binds to vascular endothelial growth factor. Acta Biomaterialia. 2005; 1:451–9. [PubMed: 16701826]
28. Hoshino Y, Nakamoto M, Miura Y. Control of Protein-Binding Kinetics on Synthetic Polymer Nanoparticles by Tuning Flexibility and Inducing Conformation Changes of Polymer Chains. Journal of the American Chemical Society. 2012; 134:15209–12. [PubMed: 22946923]
29. Nishiguchi KM, Kataoka K, Kachi S, Komeima K, Terasaki H. Regulation of pathologic retinal angiogenesis in mice and inhibition of VEGF-VEGFR2 binding by soluble heparan sulfate. PLoS One. 2010; 5:e13493. [PubMed: 20975989]
30. Muller YA, Chen Y, Christinger HW, Li B, Cunningham BC, Lowman HB, et al. VEGF and the Fab fragment of a humanized neutralizing antibody: crystal structure of the complex at 2.4 Å resolution and mutational analysis of the interface. Structure. 1998; 6:1153–67. [PubMed: 9753694]
31. Lee J-H, Canny MD, De Erkenez A, Krilleke D, Ng Y-S, Shima DT, et al. A therapeutic aptamer inhibits angiogenesis by specifically targeting the heparin binding domain of VEGF165. Proc Natl Acad Sci U S A. 2005; 102:18902–7. [PubMed: 16357200]
32. Yamazaki K, Nagao T, Yamaguchi T, Saisho H, Kondo Y. Expression of basic fibroblast growth factor (FGF-2)-associated with tumour proliferation in human pancreatic carcinoma. Virchows Archiv. 1997; 431:95–101. [PubMed: 9293890]
33. Klettner A, Roider J. Comparison of bevacizumab, ranibizumab, and pegaptanib in vitro: efficiency and possible additional pathways. Investigative ophthalmology & visual science. 2008; 49:4523. [PubMed: 18441313]
34. Nishiguchi KM, Kataoka K, Kachi S, Komeima K, Terasaki H. Regulation of pathologic retinal angiogenesis in mice and inhibition of VEGF-VEGFR2 binding by soluble heparan sulfate. PLoS One. 2010:5.
35. Taipale J, Keski-Oja J. Growth factors in the extracellular matrix. The FASEB Journal. 1997; 11:51–9. [PubMed: 9034166]
36. Ferrara N, Hillan KJ, Novotny W. Bevacizumab (Avastin), a humanized anti-VEGF monoclonal antibody for cancer therapy. Biochemical and biophysical research communications. 2005; 333:328–35. [PubMed: 15961063]

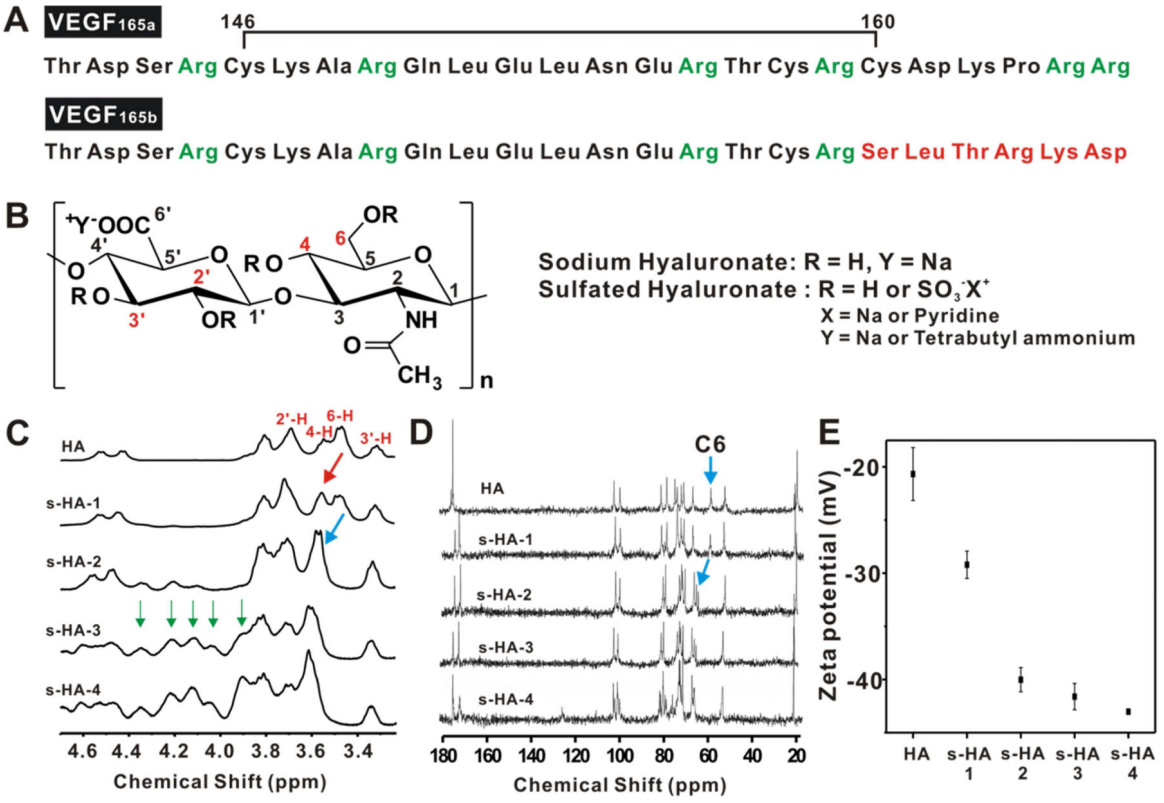

Figure 1.

Structure and characterization of $VEGF_{165a}$, $VEGF_{165b}$ and sulfated hyaluronic acid (s-HA). (**A**) The amino acid sequences of the heparin binding domains of $VEGF_{165a}$ (142-165) and $VEGF_{165b}$ (142-165) are compared, where the 6 amino acid difference between $VEGF_{165a}$ and $VEGF_{165b}$ is shown in red and the presence of a disulfide bridge in $VEGF_{165a}$ is illustrated by the black line. Positively charged arginines, which are identified in green, are important for the binding of sulfated polymers. (**B**) Chemical structures of HA and s-HA where R = H for HA and R= H or $SO_3^-X^+$ for s-HA. s-HA with different counterions were produced as illustrated. Carbons with hydroxyl groups that can be sulfated are numerically labelled in red. Carbon 6 (C6) is a reactive primary hydroxyl and most likely to be sulfated. (**C**) ^{1}H-NMR spectra (3.2 ~ 4.7 ppm) of HA and s-HAs with increasing degrees of sulfation, from s-HA-1 (least sulfated) to s-HA-4 (most sulfated). The labels in red indicate which NMR peaks correspond to which protons in HA or s-HA in Fig 1B. The peak shift of the methylene protons at C-6 from the sulfation of the hydroxyl is indicated by the red and blue arrows. Green arrows indicate proton peaks from sulfation at positions 2, 3 and 4. (**D**) ^{13}C-NMR spectra of HA and the s-HAs. The blue arrows indicate the shift of the carbon peak at C-6 (CH_2) with the sulfation of C-6 OH. (**E**) The zeta potential (mV) of HA and s-HAs. All s-HA used for zeta potential measurement were prepared using HA (150 k Da)).

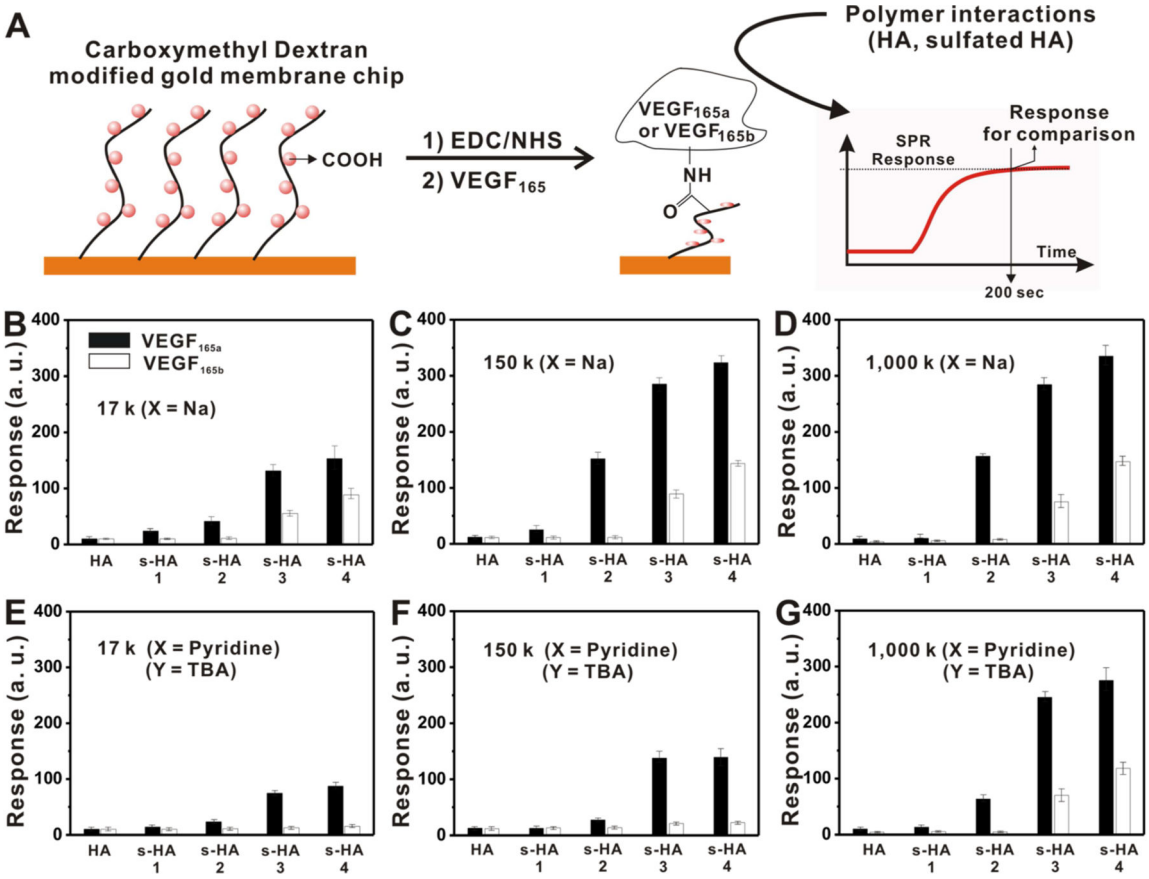

Figure 2.

Surface plasmon resonance (SPR)-based studies of HA and s-HAs binding to $VEGF_{165a}$ and $VEGF_{165b}$. (**A**) Schematic of surface modification of gold SPR chip with VEGF and SPR-based binding studies. (**B-D**) The binding response of the sodium salt of HA or s-HAs to $VEGF_{165a}$ (black bar) or $VEGF_{165b}$ (empty bar) as a function of molecular weight (17 kDa, 150 kDa, 1,000 kDa) at 200 msec after injection. (**E-G**) The binding response of pyridine and tetrabutylammonium (TBA) salts of HA or s-HAs with $VEGF_{165a}$ (black bar) or $VEGF_{165b}$ (empty bar) as a function of HA molecular weight at 200 msec after injection. The data in **Fig. 2B-G** are mean values of triplicate SPR responses obtained at 200 sec after the injection of sample solutions.

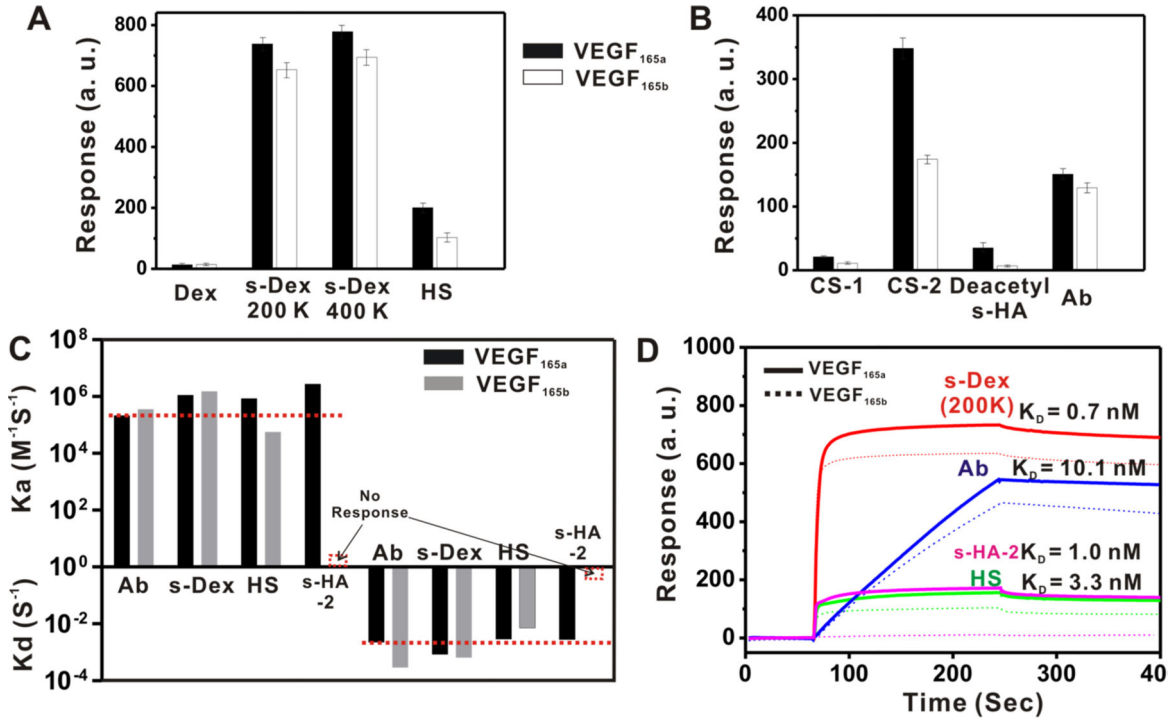

Figure 3.

Binding responses of sulfated and non-sulfated polysaccharides to $VEGF_{165a}$ and $VEGF_{165b}$. (**A**) SPR response of dextran (Dex), sulfated dextran (s-Dex 200 kDa, s-Dex 400 kDa), and heparan sulfate (HS) to $VEGF_{165a}$ (black bar) and $VEGF_{165b}$ (empty bar) are shown. (**B**) SPR response of chondroitin sulfate with a low sulfation degree (CS-1), chondroitin sulfate with a high sulfation degree (CS-2), N-deacetylated s-HA-2 (deacetyl s-HA), and anti-VEGF antibody (Ab; Avastin®) to $VEGF_{165a}$ (black bar) and $VEGF_{165b}$ (empty bar). (**C**) The calculated association rate constants (k_a) and dissociation rate constants (k_d) for the binding of anti-VEGF antibody (Ab), sulfated dextran (s-Dex, 200 kDa), heparan sulfate (HS) and s-HA-2 (150 kDa) to $VEGF_{165a}$ (black bar) and $VEGF_{165b}$ (gray bar). (D) Representative SPR sensorgrams of anti-VEGF (Ab, blue), sulfated dextran (200 kDa, red), heparan sulfate (HS, green) and s-HA-2 (150 kDa, magenta) to $VEGF_{165a}$ (solid line) and $VEGF_{165b}$ (dotted line). See Table 1 for calculation of derived constants.

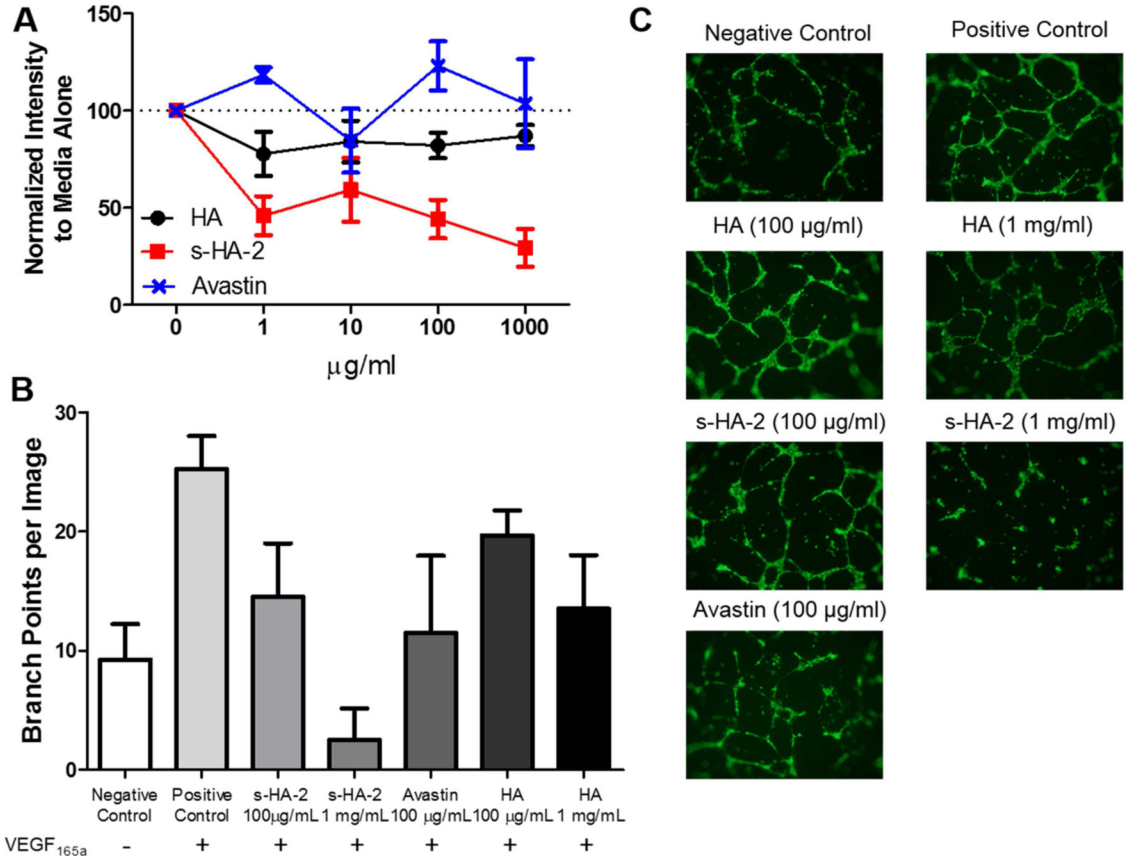

Figure 4.

Bioactivity of s-HA-2 on human umbilical vein endothelial cells (HUVECs) and human dermal microvascular endothelial cells (HMVECs). (**A**) HUVEC viability assay (CellTiter 96®Aqueous One solution cell proliferation assay ([MTS]) results in endothelial growth media (EGM-2 [which contain EBM-2, FBS, $VEGF_{165a}$, EGF, FGF-2]) in the presence of HA, s-HA-2, and Avastin® (0 – 1000 µg/mL). Data were normalized to cells in media without HA, s-HA-2 or Avastin (dotted line). s-HA-2 was significantly different from HA and Avastin at 1, 100 and 1000 µg/mL (N=4, ANOVA with Bonferroni's corrections. (**B**) Anti-angiogenic activity of s-HA-2 was evaluated by quantifying HMVEC vascular tube formation. All samples were cultured in EBM-2 media in the presence of 0.5% FBS with 100 ng/mL of $VEGF_{165a}$ except for a negative control which did not contain $VEGF_{165a}$. A representative image was taken from 4 different samples for each condition, and the average number of branch points per image was determined for each condition. All samples except HA 100 µg/mL were significantly different from the positive control of $VEGF_{165a}$ (N=4 different samples for each condition. Data are means ± standard deviations. Data were compared by one-way ANOVA with Bonferroni's corection). (**C**) Representative images from HMVEC tube formation assays. All samples except the negative control contained 100 ng/mL of $VEGF_{165a}$.

Table 1

Summary of binding constants

	K_a ($M^{-1}S^{-1}$) ($VEGF_{165a}$)	K_a ($M^{-1}S^{-1}$) ($VEGF_{165b}$)	K_d (S^{-1}) ($VEGF_{165a}$)	K_d (S^{-1}) ($VEGF_{165a}$)	K_D (nM) ($VEGF_{165a}$)
Avastin	2.2×10^5	3.6×10^5	2.2×10^{-3}	2.9×10^{-4}	10.1
s-Dex	1.1×10^6	1.5×10^6	8.5×10^{-4}	6.5×10^{-4}	0.7
HS	8.5×10^5	5.7×10^4	2.9×10^{-3}	7.2×10^{-3}	3.3
s-HA-2	2.8×10^6	N/A	2.8×10^{-3}	N/A	1.0

The rate and equilibrium binding constants (association rate constant (K_a), dissociation rate constant (K_d) and equilibrium dissociation constant (K_D)) were calculated by fitting SPR binding curves from Fig. S9-S12 with software applying an A + B = AB Langmuir binding model (values accepted when $\chi^2 \pm 100$). [27] Data are means ± standard deviation (SD), N=4.